PHYSICAL REVIEW C **73**, 061305(R) (2006)

Shell model analysis of the ^{56}Ni spectrum in the full *pf* model space

M. Horoi,[1] B. A. Brown,[2,3] T. Otsuka,[4,5] M. Honma,[6] and T. Mizusaki[7]
[1]*Department of Physics, Central Michigan University, Mount Pleasant, Michigan 48859, USA*
[2]*National Superconducting Cyclotron Laboratory, East Lansing, Michigan 48824, USA*
[3]*Department of Physics and Astronomy, Michigan State University, East Lansing, Michigan 48824, USA*
[4]*Department of Physics and Center for Nuclear Study, University of Tokyo, Hongo, Tokyo 113-0033, Japan*
[5]*RIKEN, Hirosawa, Wako-shi, Saitama 351-0198, Japan*
[6]*Center for Mathematical Sciences, University of Aizu, Tsuruga, Ikki-machi, Aizu-Wakamatsu, Fukushima 965-8580, Japan*
[7]*Institute of Natural Sciences, Senshu University, Higashimita, Tama, Kawasaki, Kanagawa, 214-8580, Japan*
(Received 7 October 2005; published 30 June 2006)

We present a full *pf*-shell spectroscopy of the low-lying states of ^{56}Ni using the GXPF1A interaction. Both the ground-state band and the first deformed band, as well as the transition probabilities, compare favorably with the experimental data. We analyze the significance of the contributions of *N*-particle *N*-hole configurations to the full model calculations, similarly to the analysis obtained for ^{28}Si in the *sd* shell some 20 years ago.

DOI: 10.1103/PhysRevC.73.061305 PACS number(s): 21.60.Cs, 27.50.+e

The wide variety of behavior observed in nuclear spectra have led to the development of an equally wide variety of theoretical models. For medium-heavy nuclei the large-basis nuclear shell model is the method of choice for encompassing all phenomena within a unified theory. With advances in the computational technology the scope and precision of this method can be continually increased. In this rapid communication we report on results for ^{56}Ni at the forefront of computational technology in which single-particle, collective and chaotic behaviors find a unified interpretation. We use the GXPF1A interaction [1] in the full *pf* model space. We show the evolution of the theoretical spectra as a function of the maximum number of nucleons excited out of the $0f_{7/2}$ orbit. We also show how a qualitative interpretation of low-lying states in terms of configurations with a specific number of excitations can be made. These calculations involve state-of-the art computations for M-scheme basis dimensions up to 10^9 carried out at the new High Performance Computer Center at MSU.

The large-basis shell-model description of nuclei around ^{56}Ni is at the forefront of our microscopic understanding of nuclear properties. In the simplest model the $0f_{7/2}$ (denoted in the following by f) orbit is filled with 16 nucleons and the next few unfilled orbits are $1p_{3/2}$, $1p_{1/2}$, and $0f_{5/2}$ (denoted in by r). The historical development of configuration mixing in this region can be related to truncations in terms of the partitions $f^{n-t}r^{m+t}$, where n is the maximum number of nucleons allowed in the f orbit, m is the minimum number of nucleons allowed in the r orbits ($n = 16$ and $m = 0$ for ^{56}Ni), and t is the maximum number of nucleons allowed to be excited from f to r. The earliest calculations were obtained with Hamiltonians designed for small t values. For example, a qualitative understanding of the ground states of ^{55,56,57}Ni with $t = 0$ and excited states in ^{56}Ni with $t = 1$ may be obtained [2]. However, there are many other low-lying states in ^{56}Ni that require a much more complete basis. In the high resolution ^{58}Ni$(p, t)^{56}$Ni experiment [3] eight 0^+ states are observed up to 10 MeV. In high-spin γ spectroscopy a deformed band has been observed ending at a 2^+ state at 5.35 MeV [4]. In analogy with the low-lying deformed band in ^{16}O, this band in ^{56}Ni might be understood in terms of the states for four particles excited from f to r ($4p$-$4h$), and in Ref. [5] this idea was refined to $4p$-$4h$ relative to the correlated ^{56}Ni ground state. In the (p, t) experiment [3] the 0^+ state at 5.01 MeV was suggested to be the predominantly $4p$-$4h$ state, however no interpretation could be made for the lower 0^+ state at 3.95 MeV.

We focus on the complete *pf*-shell spectroscopy of ^{56}Ni up to about 10 MeV and how it can be understood in terms of simpler underlying configurations. It is now known that a consistent interpretation can be obtained only in a model space that goes up to very high t [6] with a Hamiltonian designed for this high-t model space. In Ref. [4] a basis with $t = 6$ was used with a KB3 Hamiltonian [7] that was modified to put the deformed band in the correct location, whereas in a larger basis with the FPD6 interaction [8] the deformed band comes in about the right location [6]. The most recent effective Hamiltonians GXPF1 [9,10] and GXPF1A [1] are derived from a microscopic calculation by Hjorth-Jensen based on renormalized G-matrix theory with the Bonn-C interaction [11] and are refined by a systematic fitting of the important linear combinations of two-body matrix elements to low-lying states in nuclei from $A = 47$ to $A = 66$, including some states in the ^{56}Ni, in a model space that in principle goes to $t_{\max}$, although in practice involves some approximations [9]. Shell-model calculations that focus on the properties of the shape coexistence of the ground-state and deformed bands in ^{56}Ni were presented previously [12,13]. The GXPF1 interaction was used in Ref. [14] in a truncated basis with $t = 6$.

Calculations have been carried out using the public version of the ANTOINE code [15] and the CMICHSM code [16]. In particular, for low spins we took advantage of the reduced effective dimension associated with time reversal symmetry that is implemented in the ANTOINE code. For higher spins we used the CMICHSM code's spin projection techniques as described in Ref. [16].

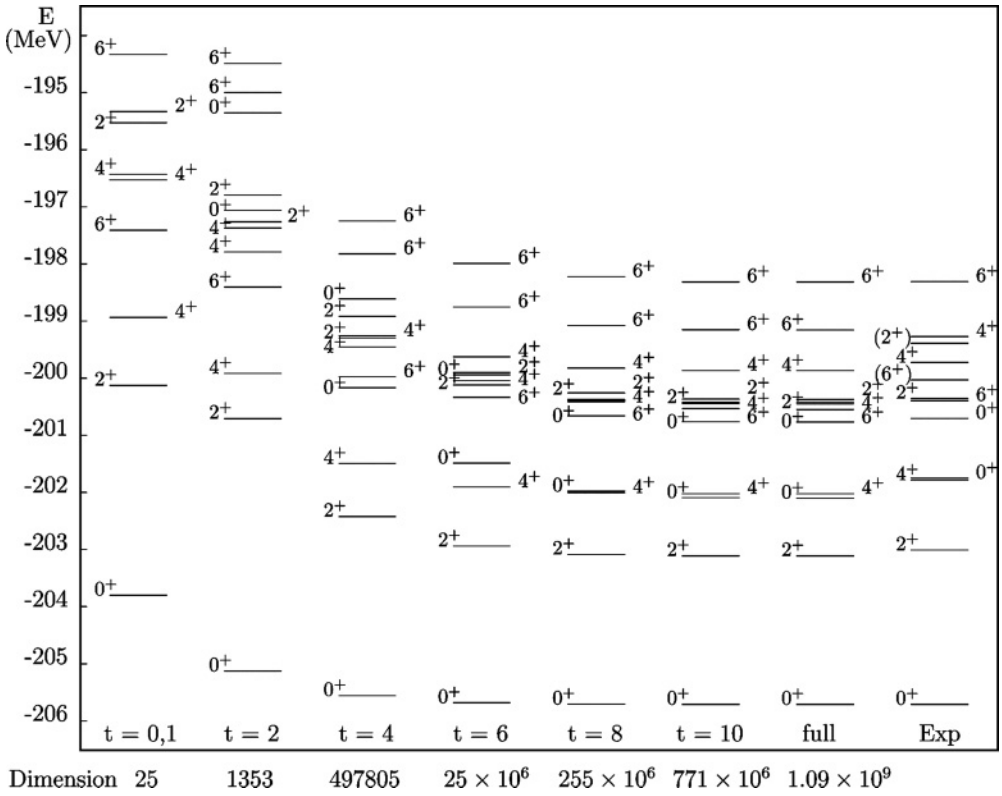

FIG. 1. The evolution of the first three 0^+, 2^+, 4^+, and 6^+ states as a function of the truncation level t.

Figure 1 shows the evolution of the first three 0^+, 2^+, 4^+, and 6^+ states as t increases. This is similar to the analysis that was shown for ^{28}Si in the *sd* shell 20 years ago; see Fig. 1 in Ref. [17]. The experimental excitation energies are from Ref. [18]. One can observe that the calculations are practically converged at the $t = 10$ level of approximation. The largest energy deviation between the full model calculations and the $t = 10$ calculations was 0.014 MeV for the second 2^+ state. Calculations for ^{56}Ni excited 0^+ states based on truncations that stopped at $t = 2$ or $t = 4$ [19,20] had difficulty reproducing the experiment levels, and we can see in Fig. 1 that the spectra at this level of truncation are far from convergence.

Figure 2 shows the spectra obtained with a specific number of particles t_o excited from f to r, that is, t_o p-$t_o h$ configurations. The energies of the configurations are shifted down by $(t_o \times \delta G)$ with $\delta G = 0.9$. δG represents the change in the effective f-r single-particle gap when going from the full-space wave functions for the ^{56}Ni ground state to the closed-shell ($t_o = 0$) ground state. The value of δG is obtained empirically by comparing the $t_o = 0$ energies of ^{55,56,57}Ni calculated with the GXPF1A interaction with the experimental values. From Fig. 2 we can understand the origin of low-lying states in terms of the pure t_o configurations. The $t_o = 2$ spectrum shows a two-phonon character with the lowest state turning out to be 0^+. The next lowest states are those from $t_o = 4$, with the lowest few states clearly showing a rotational pattern. States for $t_o > 4$ that start around 8 MeV or higher are not shown.

In the full configuration spectrum of Fig. 1 the 0^+ ground state is predominantly (50%) $t_o = 0$ and the first excited 2^+ state is predominantly $t_o = 1$. The states that are predominantly $t_o = 1$ have almost converged at $t = 6$. However, the excited deformed band corresponding to the predominantly

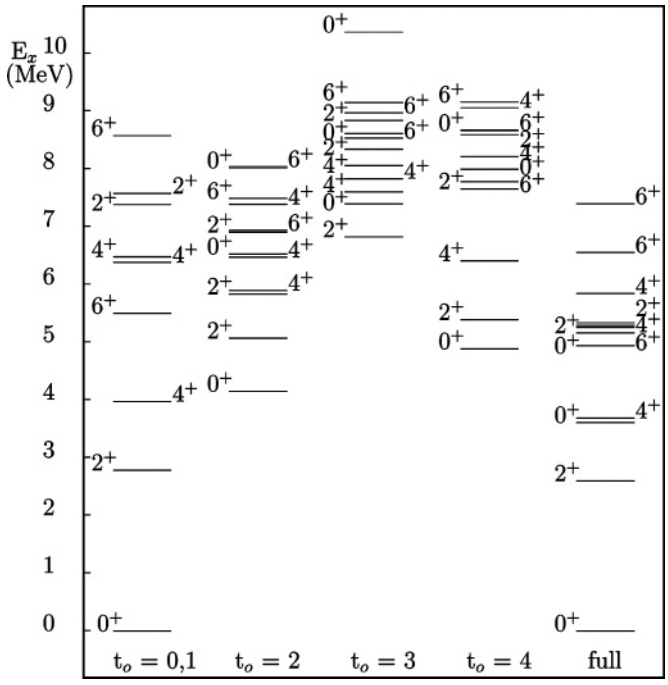

FIG. 2. The first three 0^+, 2^+, 4^+, and 6^+ states for the pure t_o configurations.

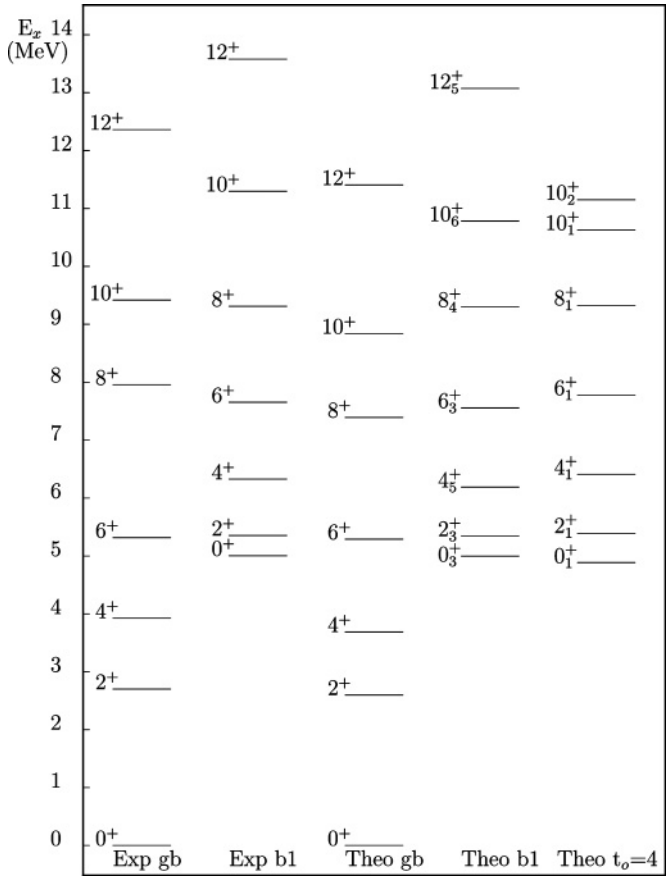

FIG. 3. Experimental and theoretical spectra for the ground band (gb) and the first rotational band (b1). The experimental energies are taken from Ref. [4].

$t_o = 4$ configuration does not converge until $t = 10$; that is, $\delta t = 6$ on top of initial $t_o = 4$. The 0^+ deformed band head first appears in the spectrum for $t = 4$ at around 7 MeV and it slowly converges to 5.2 MeV in excitation at $t = 10$.

The t_o truncations provide an estimate of the level density with calculations that are trivially small in size compared to the full *pf* model space. The $t_o = 2$ spectrum has six excited 0^+ $T = 0$ and three 0^+ $T = 1$ states up to 10 MeV (the lowest three $T = 0$ states are shown in Fig. 2). The lowest 0^+ $T = 1$ comes at 7.77 MeV compared to its experimental values of 7.91 MeV [18]. The lowest 0^+ $T = 2$ comes at 10.24 MeV to be compared with states observed [18] at 9.94, 10.01, and 10.03 MeV that can be interpreted in terms of isospin mixing of the $T = 2$ state into $T = 0$ states. There are several $t_o = 2$, 0^+ $T = 0$ within 100 keV of the $T = 2$ state. These $2p$-$2h$ states are the type of states expected to be reached in the (p, t) reaction from pickup of two neutrons from the $0f_{7/2}$ orbit in ^{58}Ni. The number of 0^+ seen in the (p, t) experiment [3] is consistent with theory. The $t_o = 1, 2$ spectra has a total of about 160 states up to 10 MeV in comparison with about 50 seen in (p, t) (some of which may be negative parity). Including $t_o = 3 - 5$ there are about 300 states up to 10 MeV.

Figure 3 shows the experimental and theoretical $t = 10$ spectra for the ground band (gb) and the first rotational band (b1) [4]. The experimental energies are taken from Ref. [4].

TABLE I. Electromagnetic properties of the states in the deformed band obtained in the $t = 10$ model space. The units are e fm^2 for the electric quadrupole moments and e^2 fm^4 for the $J \to J - 2$ $B(E2)$ values.

J_n	E_x (MeV)	$\langle Q \rangle_{J0}$	$(Q_0)_{\rm sp}$	$B(E2)$	$\lvert Q_0 \rvert_{\rm tr}$
2_3	5.342	−41.6	+145.3	413.2	144.1
4_5	6.027	−55.2	+151.9	598.0	143.8
6_3	7.556	−56.2	+140.6	609.3	139.5
8_4	9.300	−47.2	+112.2	558.4	130.5
10_6	10.782	−63.9	+147.0	591.1	132.5
12_5	13.071	−62.7	+141.1	612.3	133.7

The states in the first rotation band were identified by the large quadrupole moment matrix element $\langle Q \rangle_{J0}$, and by the large $B(E2; J \to J - 2)$ values between states in the band. We use effective charges of $e_{\rm eff}(\pi) = 1.5\,e$ and $e_{\rm eff}(\nu) = 0.5\,e$. These effective charges that come from the admixtures of the giant quadrupole states outside the *pf* model space [21] are close to the one extracted from the experiment and to those suggested by a multi-major-shell calculation [22]. The oscillator parameter used was 2.04 fm. We also checked if the values of the spectroscopic intrinsic quadrupole moment $(Q_0)_{\rm sp}$,

$$\langle Q \rangle_{JK} = \frac{3K^2 - J(J+1)}{(J+1)(2J+3)} (Q_0)_{\rm sp}, \tag{1}$$

obtained under the assumption that these states belong to a $K = 0$ rotational band [23] is consistent with the value of the corresponding transitional intrinsic quadrupole moment extracted from the $B(E2)$ probabilities within the rotational band,

$$B(E2; J \to J-2) = \frac{15}{32\pi} \frac{J(J-1)}{(2J+1)(2J-1)} (Q_0)^2_{\rm tr}. \tag{2}$$

The results for the $t = 10$ model space are summarized in Table I. We checked, however, some of these results in the full space, and we found an increase of less than 2%.

The emergence of the rotational band is clearly seen in Fig. 4, which shows all relevant $B(E2)$ values for all states up to the rotational band. The rotational band is nonyrast and is embedded in a set of "chaotic" states of the same spin that are connected to each other by much smaller $B(E2)$ values. The only other large $B(E2)$ value that appears in Fig. 4 is the one connecting the second 0^+ state with first 2^+ state. This large $B(E2) = 550\,e^2$ fm^4 (corresponding to mean lifetime of 0.04 ps) arises from the two-phonon character of this state as noted in the previous discussion for the $t_o = 2$ spectrum of Fig. 2. The low-lying 0^+ states in the $t = 10$ calculation are at 3.61, 4.94, 6.16, and 6.82 MeV. The energies are in good agreement with those observed at 3.92, 5.00, 6.0*, and 6.66 MeV, where the (*) indicates a level observed only in ^{54}Fe(^{3}He,t) [24].

The status of the 0^+, $T = 0, 1, 2$ states in ^{56}Ni is clarified by this work. Our calculation suggests that the rotational band head is the third 0^+ state found at 5.01 MeV in (p, t) experiments [3]. The rotational band observed experimentally around 9 MeV [4] does not come out of the *pf* model space

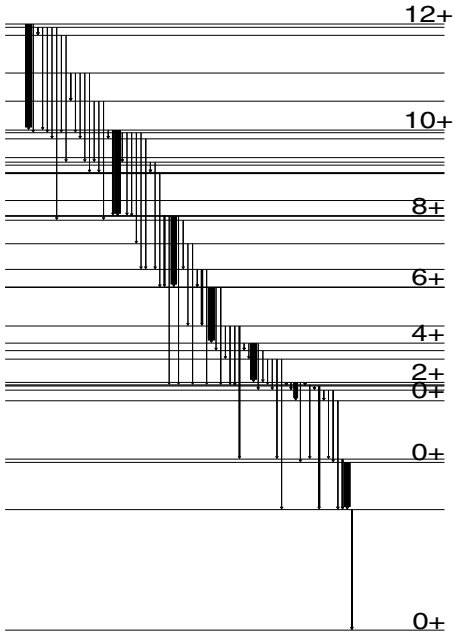

FIG. 4. Calculated $B(E2)$ values over 20 $e^2\text{fm}^4$ that connect the even-J states up to and including those in the deformed band shown in Fig. 3. The widths of the arrows are proportional to the $B(E2)$ value with the largest being 600 $e^2\text{fm}^4$. The states with the largest $B(E2)$ values are labeled by their J value.

and it is likely related to excitation into the $0g_{9/2}$ orbit that is outside of our model space. The two-phonon structure of the second 0^+ state should be confirmed experimentally from a lifetime measurement. We predict about 300 *pf*-shell levels (all J and T) up to 10 MeV. In this rapid communication we have focused on the properties of even-spin states. But we note the lowest odd-spin state in the full-space model is a 3^+ state at 4.75 MeV. A new experimental investigation may give information on these low-lying odd-spin states [25].

A new experimental study of the spectroscopy of ^{56}Ni has been recently published [14]. It contains a shell-model analysis using the GXPF1 interaction, but it stops at the $t = 6$ level of approximation. Our Fig. 1 clearly shows that the spectrum of ^{56}Ni is not yet converged at the $t = 6$ level of approximation. In particular, at this level of approximation the deformed band is not sufficiently well described: the 0_3^+ band head is not at the right location (see also Fig. 6 of Ref. [14]) and the members of the band cannot be accurately identified. Our Figs. 3 and 4, as well as Table I, clearly identify the collectivity of the states in the band, which compares well with the experimental data of Ref. [4]. We also looked into the decay pattern of the nearby 8^+ states at experimentally 7.95 and 8.22 MeV analyzed at length in Ref. [14]. Our calculations for the 8^+ decays are similar to those found in Ref. [14] indicating that the levels are crossed in the theory compared to experiment (but still within the typical level to level deviation).

The authors acknowledge support from NSF grant PHY-0244453. This work was supported in part by a Grant-in-Aid for Specially Promoted Research (13002001) from the MEXT of Japan. The authors acknowledge computational resources provided by the Michigan State University High Performance Computing Center and the Research Excellence Fund of the State of Michigan for support of the HPC cluster at CMU.

[1] M. Honma, T. Otsuka, B. A. Brown, and T. Mizusaki, Eur. Phys. J. A **25** Suppl. 1, 499 (2005).
[2] G. Kraus *et al.*, Phys. Rev. Lett. **73**, 1773 (1994).
[3] H. Nann and W. Benenson, Phys. Rev. C **10**, 1880 (1974).
[4] D. Rudolph *et al.*, Phys. Rev. Lett. **82**, 3763 (1999).
[5] T. Mizusaki, T. Otsuka, M. Honma, and B. A. Brown, Phys. Rev. C **63**, 044306 (2001).
[6] T. Otsuka, M. Honma, and T. Mizusaki, Phys. Rev. Lett. **81**, 1588 (1998).
[7] A. Poves, J. Sanchez-Solano, E. Caurier, and F. Nowacki, Nucl. Phys. **A694**, 157 (2001).
[8] W. A. Richter, M. G. van der Merwe, R. E. Julies, and B. A. Brown, Nucl. Phys. **A523**, 325 (1991).
[9] M. Honma, T. Otsuka, B. A. Brown, and T. Mizusaki, Phys. Rev. C **65**, 061301(R) (2002).
[10] M. Honma, T. Otsuka, B. A. Brown, and T. Mizusaki, Phys. Rev. C **69**, 034335 (2004).
[11] M. Hjorth-Jensen, T. T. S. Kuo, and E. Osnes, Phys. Rep. **261**, 125 (1995).
[12] T. Mizusaki, T. Otsuka, Y. Utsuno, M. Honma, and T. Sebe, Phys. Rev. C **59**, R1846 (1999).
[13] T. Mizusaki, T. Otsuka, M. Honma, and B. A. Brown, Phys. Rev. C **63**, 044306 (2001).
[14] E. K. Johansson *et al.*, Eur. Phys. J. A **27**, 157 (2006).
[15] E. Caurier, shell model code ANTOINE, IRES, Strasbourg 1989–2004; E. Caurier and F. Nowacki, Acta Phys. Pol. **30**, 705 (1999).
[16] M. Horoi, B. A. Brown, and V. Zelevinsky, Phys. Rev. C **67**, 034303 (2003).
[17] B. A. Brown and B. H. Wildenthal, Ann. Rev. Nucl. Part. Sci. **38**, 29 (1988).
[18] www.nndc.bnl.gov
[19] G. Oberlechner and J. Richert, Nucl. Phys. **A191**, 577 (1972), and references therein.
[20] H. Nakada, T. Sebe, and T. Otsuka, Nucl. Phys. **A571**, 467 (1994).
[21] B. A. Brown, A. Arima, and J. B. McGrory, Nucl. Phys. **A277**, 77 (1977).
[22] P. Navratil, M. Thoresen, and B. R. Barrett, Phys. Rev. C **55**, R573–R576 (1997).
[23] A. Bohr and B. Mottelson, *Nuclear Structure* (W. A. Benjamin, New York, 1975), Vol. II.
[24] H. Fuchs *et al.*, Phys. Lett. **B49**, 447 (1974).
[25] N. Pietralla (private communication).